HHS Public Access

Author manuscript

Dev Biol. Author manuscript; available in PMC 2019 June 01.

Published in final edited form as:

Dev Biol. 2018 June 01; 438(1): 23–32. doi:10.1016/j.ydbio.2018.03.012.

The cellular prion protein promotes olfactory sensory neuron survival and axon targeting during adult neurogenesis

Lindsay E Parrie[*], **Jenna AE Crowell**, **Glenn C Telling**[*], and **Richard A Bessen**

Prion Research Center; Department of Microbiology, Immunology, and Pathology; Colorado State University; Fort Collins, Colorado, United States of America

Abstract

The cellular prion protein (PrP^C) has been associated with diverse biological processes including cell signaling, neurogenesis, and neuroprotection, but its physiological function(s) remain ambiguous. Here we determine the role of PrP^C in adult neurogenesis using the olfactory system model in transgenic mice. Olfactory sensory neurons (OSNs) within the olfactory sensory epithelium (OSE) undergo neurogenesis, integration, and turnover even into adulthood.

The neurogenic processes of proliferation, differentiation/maturation, and axon targeting were evaluated in wild type, PrP-overexpressing, and PrP-null transgenic mice. Our results indicate that PrP^C plays a role in maintaining mature OSNs within the epithelium: overexpression of PrP^C resulted in greater survival of mitotically active cells within the OSE, whereas absence of prion protein resulted in fewer cells being maintained over time. These results are supported by both quantitative PCR analysis of gene expression and protein analysis characteristic of OSN differentiation. Finally, evaluation of axon migration determined that OSN axon targeting in the olfactory bulb is PrP^C dose-dependent. Together, these findings provide new mechanistic insight into the neuroprotective role for PrP^C in adult OSE neurogenesis, whereby more mature neurons are stably maintained in animals expressing PrP^C.

Keywords

prion; proliferation; differentiation; axon targeting

Introduction

Adult neurogenesis is comprised of several, often concomitant, developmental processes. Similar to early development, it begins with proliferation of progenitor cells, followed by differentiation into a neuronal lineage and maturation into a neuronal cell phenotype. The final neurogenic phase is for the newly born neuron to make appropriate, functional synaptic connections. If the cell fails to complete any of these steps, it is not maintained.

[*]Corresponding author: 1619 Campus Delivery, Fort Collins, CO 80523, Tel.: (970) 491-7343, lparrie@colostate.edu; 1619 Campus Delivery, Fort Collins, CO 80523, glenn.telling@colostate.edu.

Olfactory sensory epithelium (OSE) is one of only a few sites of continual adult neurogenesis (Murray and Calof, 1999). This epithelium is a useful *in vivo* system for investigating mechanisms that regulate neurogenesis because it is comprised of only one neuron type (the olfactory sensory neuron, OSN) and one support cell type: the sustentacular cells (Farbman 1992). These neurons extend between the periphery to the central nervous system, contacting both the external environment as well as circuits extending throughout the brain. Neurogenesis within the OSE occurs continuously in response to normal turnover, as mature neurons have a limited lifespan of approximately 30–90 days, on average (Graziadei and Graziadei 1979, Mackay-Sim and Kittel 1991), although some may live upwards of 12 months (Hinds et al. 1984). Therefore, mature OSNs exist adjacent to developing neurons and provides a system with unique opportunities to study the processes of neuronal integration into existing circuitry.

The cellular prion protein (PrP^C) is predominantly recognized from its requirement in rapidly progressing transmissible spongiform encephalopathies (TSEs) including human Creutzfeldt-Jacob disease and cervid chronic wasting disease. It is now recognized that expression of PrP^C plays various roles, including protection against cellular stress, cell signaling, and regulating neurogenic processes (Legname 2017). Although much work has been done to elucidate the normal cellular function(s) of PrP^C, there are relatively few *in vivo* studies addressing its role(s). From these studies, we know that PrP^C is important in pro-neurogenic processes, including promotion of stem cell proliferation within the subventricular zone (SVZ) and differentiation of those newly generated cells into a neuronal cell fate (Steele et al. 2006). Others have reported that neurogenesis in the dentate gyrus can partially preserve hippocampal function during murine prion infection (Gomez-Nicola et al. 2014). PrP^C is also important in the neurogenic process of axon elongation, presumably through regulating cell adhesion processes (Málaga-Trillo et al. 2009, Bodrikov et al. 2011, Huc-Brandt et al. 2014). Expression of PrP^C is essential for adherens junction stability, promotes Fyn-Reggie cell-signaling, and alters cytoskeletal composition, thereby promoting neurite formation and growth cone elongation. However, perhaps due to often conflicting effects of PrP^C in adjacent cell types, such as glia vs. neurons (Mehrabian et al. 2015), results in whole brain tissues may be difficult to interpret or even obscured. Therefore, the OSE also represents a relatively isolated, homogenous neuronal population in which to perform analysis of neurogenesis and differentiation using developmental markers, which have been well characterized (McIntyre et al. 2010, see also Fig. 3). Expression of PrP^C at high levels within the olfactory sensory neuron suggests a role in olfaction, and possibly a role in the development of these neurons (Le Pichon and Firestein 2008, Dibattista et al. 2011). Additionally, these neurons accumulate and shed infectious prions during disease (Zanusso et al. 2003, Bessen et al. 2010). Elucidating the cellular function PrP^C is of importance in understanding mechanisms of neurogenesis and devising efficacious therapeutics for neurodegenerative prion disease.

In order to fully elucidate the role of PrP^C in adult neurogenesis, we modulated PrP^C expression levels under homeostatic conditions using PrP-knockout and -overexpressing transgenic mice on two separate congenic backgrounds. We use this *in vivo* model to study the effects of PrP^C dose on the neurogenic processes of proliferation, differentiation and maturation, and axon targeting. Temporal analysis of olfactory neurogenesis illuminates

subtle effects of the loss or gain of function of the cellular prion on adult neurogenesis and cell survival in discrete subsets of neurons.

Material and Methods

Animals

We used 2.5 month-old male and female wild type FVBCr/N mice and congenic PrP-KO (Zurich I line) and PrP-OE ($Tg4112^{+/+}$) mice for proliferation and differentiation studies (Prion Research Center, CSU, Fort Collins, CO). For axon tracing, B6;129P2-$Olfr17^{tm1Mom}$/MomJ mice (Jackson Laboratories, Bar Harbor, ME) were used, along with and Edinburgh PrP-KO line on a B6 background (kindly provided by Rocky Mountain Laboratories, Hamilton, MT). Tg4112 mice were interbred with the B6 mice for 10 generations for the tracing experiments. All animals were bred and maintained by the laboratory animals in research facility and all protocols were approved in accordance with the Colorado State University IACUC committee guidelines.

BrdU Treatment and Tissue Collection

To quantify proliferation and survival in the OSE, the thymidine analog 5′-bromodeoxyuridine (BrdU) (Sigma-Aldrich, St. Louis, MO) was administered as three pulse labels (three i.p. injections, 2 hrs apart; 50 mg/kg of body weight, in sterile saline). Animals were perfused 1, 7, or 14 days after the last BrdU administration (n=3 per timepoint). These collections correspond with developmentally important timepoints and were used to determine proliferation and survival of newly born OSNs. Animals were deeply anesthetized with isoflurane (MWI Veterinary Supply, Boise, ID) and were transcardially perfused with 0.1 M PBS followed by periodate-lysine-paraformaldehyde (PLP) fixation (McLean and Nakane 1974). Nasal turbinates were postfixed in PLP 24 hrs before decalcification in 10% formic acid and paraffin embedding. Coronal sections were cut at 4 μm thick using standard methods.

Histology

For BrdU, all immunohistochemical procedures were performed on a minimum of every sixth slide to prevent quantification of the same nucleus across adjacent sections. 6 slides, each with 2–4 tissue sections, were quantified per animal. Sections were rehydrated in a graded alcohol series and quenched in 1% peroxidase. BrdU antigen retrieval was completed in 1M HCl for 15 min at 37°C. Samples were then rinsed in 1× TBS and blocked sequentially in 20% Streptavidin/10% normal donkey serum (NDS), 20%Biotin/10%NDS, and 20 ug/mL Donkey anti Mouse (Fab) Ig fragments (Jackson Immuno-Research Laboratories, West Grove, PA, AntibodyRegistry: AB_2307338) in 0.5% Triton X-100 in TBS (TBST). The primary antibody (Bu20a mouse anti-BrdU monoclonal, 1:400; Cell Signaling, Danvers, MA, AB_10548898) was applied overnight at 4°C in a blocking solution of 3% NDS (all sera available from Jackson ImmunoResearch)/TBST, followed by a series of TBST rinses and incubation in the secondary antibody (donkey-anti-mouse-biotinylated, 3 μg/ml; Jackson ImmunoResearch, AB_2307438) in blocking solution at room temperature for 1 hr. Streptavidin-horseradish peroxidase (HRP) (Biosource International, Camarillo, CA) was used at 1:800 and incubated at room temperature for 20 min. BrdU was

then visualized with localization of HRP activity with DAB+ chromogen (Dako, Carpinteria, CA). Prion localization was done as above, using 98% Formic Acid antigen retrieval and mouse-anti-PrP (SAF-32, Cayman Chemical 189720, AB_327961) and horse-anti-mouse-bt (Vector Laboratories, Burlingame, CA, AB_2336180) antibodies for detection.

Dual immunofluorescence for BrdU was combined with that of either GAP43 or OMP. The primary antibodies used included: mouse-anti-BrdU (1:150, Cell Signaling) and rabbit-anti-Gap43 (1:250, EMD Millipore, Darmstadt, Germany, AB_612169) or goat-anti-OMP (1:250, Wako Chemicals, Richmond, VA, AB_664696) in a blocking solution of 10% normal horse serum in TBST. Detection of OSN-specific primary antibodies was performed by incubation with goat-anti-rabbit-AF568 (10ug/ml, Life Technologies, AB_143011) or donkey-anti-goat-AF568 (1.1 μg/ml, Life Technologies, AB_142581) at room temperature for 2 hours. To detect the BrdU primary, sections were incubated with donkey-anti-mouse-bt (2.4 μg/ml) in blocking solution containing 10% normal horse serum and 3% normal hamster serum in TBST for 30 minutes and with streptavidin-AF488 (1:400, ThermoFisher, AB_2315383) for a final 30-minute incubation. Samples were mounted using MOWIOL 4-88 (EMD Millipore) and coverslips appropriate for fluorescent confocal microscopy (Fisher, Pittsburgh, PA). The tyrosine hydroxylase immunofluorescent labeling was done as above, using rabbit-anti-TH (1:250, EMD Millipore, AB_696697) and a goat-anti-rabbit-bt (1.1 μg/ml, Vector, AB_2313606) with streptavidin-AF488 for detection (n=4 KO, WT, n=5 OE, 2-4 slides per animal). Comparisons between wild type, PrP KO, and PrP OE animals were completed using ANOVA, with TukeyKramer HSD post hoc multiple comparisons. All data are presented as mean+/−S.E. and the level of significance was set at $P<0.05$ for all statistical analyses. Post-processing for color and contrast on any images was completed with Adobe Photoshop software after any analysis was performed.

Quantitative Real-Time PCR

Total RNA was isolated from nasal turbinates of 8 animals per treatment using TRIzol reagent (Invitrogen) according to the manufacturer's protocol. Total RNA was resuspended in 60 ul of nuclease-free water. Nucleotide concentration was determined by absorbance at 260 nm and 3.5 μg was used for 20 μl-cDNA synthesis reactions using AMV reverse transcriptase (Fisher Scientific) and Oligo(dT)12–18 primer (Life Technologies) as described previously (Parrie et al. 2013). Resulting cDNA was treated with RNase H (New England Biolabs, Ipswich, MA) to remove complementary RNA.

Primers were designed for the following genes—*Actb* (actin, beta) [GenBank Accession NM_007393, F: 5′-TGT GAT GGT GGG AAT GGG TCA GAA-3′, R: 5′-TGT GGT GCC AGA TCT TCT CCA TGT-3′]; *Bmp4* (Bone morphogenetic protein 4) [GenBank Accession NM_007554, 48F: 5′-ATC AGG AGA TGG TGG TAG AG-3′, 49R: 5′-AGT TTG TGT GGT ATG TGT AGG-3′]; *Cnga2* (Cyclic nucleotide gated channel alpha 2) [GenBank Accession NM_007724, F: 5′-GAA GCT CAA ACA GCG CAT CAC AGT-3′, R: 5′-ACA GGC ACC TAT GGC TAT TCA GCA-3′]; *Cxcr4* (Receptor 4 chemokine (C-X-C)) [GenBank Accession NM_009911, F: 5′-AGC TAA GGA GCA TGA CGG ACA AGT-3′, R: 5′-AAC GCT GCT GTA GAG GTT GAC AGT-3′]; *Dbn1* (Drebrin 1 transcript variant 1) [Genbank Accession NM_001177371, F: 5′-TTT GAA CAG GAA

CGG ATG G-3′, R: 5′-ACC TCC TCT TGG CTT CTT-3′]; *Dpysl3* (Dihydropyrimidinase-like 3) [GenBank Accession NM_009468, F: 5′-AAG GAA ATG TGG TCT TTG GCG AGC-3′, R: 5′-TGG CCA GCA AGG AGT TGA TGT AGT-3′]; *Eif1a* (Eukaryotic translation initiation factor 1A) [GenBank Accession NM_010120, F: 5′-CAA CAC TGT TTG CTG CCT GTG GAT-3′, R: 5′-ACA GCA GCT GAG ACT CCT TTC CAA-3′]; *Gap43* (Growth associated protein 43) [GenBank Accession NM_008083, F: 5′-ATA AGG CTC ATA AGG CTG CGA CCA-3′, R: 5′-TCC TTC TTC TCC ACA CCA TCA GCA-3′]; *IgSF8* (immunoglobulin superfamily, member 8) [GenBank Accession NM_080419.1, F: 5′-CAC AGT CTA CCC CTA CAC GC-3′, R: 5′-GGT GCT ACA GAT CAC CGC TT-3′)]; Npy () [GenBank Accession NM_023456.2, F: 5′- GGT AAC AAG CGA ATG GGG CT-3′, R: 5′-ATG TAG TGT CGC AGA GCG GA-3′]; *Omp* (Olfactory marker protein) [GenBank Accession NM_011010, F: 5′-ATT GAG CTG GTA CTG GCT TGT GGA-3′, R: 5′-AAA TGC CAG CCT TCC TAA CAG GGA-3′]; *Prnp* (Prion protein) [GenBank Accession NM_011170, F: 5′-CAT GAG CAG GCC CAT GAT CCA TTT-3′, R: 5′-TGC ACG AAG TTG TTC TGG TTG CTG-3′]; *Snai2* (Snail family zinc finger 2) [GenBank Accession NM_011415.2, F: 5′-TCC TCA CCT CGG GAG CAT AC-3′, R: 5′-GGA CTT ACA CGC CCC AAG GA-3′].

Quantitative analysis was conducted using BioRad SsoFast™ EvaGreen® Supermix and CFX96 thermal cycler. Triplicate 20 μl reactions for each animal each consisted of 1 μl first-strand cDNA, 10 μl 2× EvaGreen® Master Mix, 0.25-1 μl each of forward primer and reverse primer (at 10 mM starting concentration), and 7 μl PCR grade water. PCR conditions included an initial denaturation at 95°C for 30 s, followed by 35-40 cycles of denaturation at 95°C for 7 s and annealing/extension at 59-62.5°C for 20 s. At the end of each run, an analysis of the PCR product melting temperature was conducted. Amplicon specificity was also verified by sequencing. Transcript concentrations were calculated with BioRad software using standard curves produced by serial dilution of purified PCR product (1 ag/ml to 10 ng/ml). Use efficiencies for all reactions were confirmed to be between 1.86 and 1.96 and PCR amplicons were confirmed by sequencing. Statistical analysis was performed using GraphPad Prism software (LaJolla, CA) in which log-transformed means for transcript abundance were compared between wild type, PrP KO, and PrP OE animals using ANOVA. Post hoc multiple comparisons were made using TukeyKramer HSD tests. Data are presented as the difference between the total average log copy number of KO or OE as compared to wild type +/−standard error of the difference between means and the level of significance was set at $P<0.05$.

Western Blot Analysis

Tissue collection and western blot were performed as described previously (Bessen et al. 2012), with the following modifications. Briefly, 40 μg of 10% nasal turbinate homogenates from 6 animals per genotype were analyzed on MOPS (moprholinepropanesulfonic acid) NuPAGE gels (12% acrylamide; Life Technologies), and transferred to polyvinylidene difluoride (0.45 μm PVDF) membranes specific for fluorescence detection (Immobilon-FL, EMD Millipore, Taunton, MA). For analysis of GAP43, rabbit-anti-Gap43 (EMD Millipore) antibody was used at 0.4 μg/ul. OMP was detected with goat-anti-OMP polyclonal antibody (Wako Chemicals) at a 1:5000 dilution. PrP^{C} was detected with human-anti-PrP (D18, in

house) at 0.05ug/ml. For detection of GAPDH, chicken-anti-GAPDH antibody (EMD Millipore, AB_10615768) was used at 0.33 μg/ml. The secondary antibodies used were IRDye conjugates available from LI-COR (Lincoln, NE): 800CW Dky Anti-Goat IgG (AB_621846), 680RD Dky Anti-Rabbit IgG (AB_10954442), 800CW Gt Anti-Human IgG (AB_10806644), and 680RD Dky Anti-Chicken IgG (AB_10974977), all at concentrations of 0.02 μg/ml. Blots were visualized on the Odyssey CLx Imager system (LI-COR) and associated Image Studio 4.0 software was used to measure the total signal, with OMP and GAP43 signal normalized to the GAPDH signal within the lane. Statistical analysis was performed using Student's *t*-test, with *P* values of <0.05 considered significant.

Labeling and quantification of P2 OSN Axons

Wholemount processing was carried out as described in Schaefer et al. 2001 with the following differences. 10-week-old male and female B6;129P2-Olfr17^{tm1Mom}/MomJ (commonly called P2-IRES-tau-lacZ mice, available from the Jackson Laboratory) on a mixed C57BL/6 129 background were used (n>8 per genotype). Mice were processed in batches of mixed genotypes, to account for staining efficiency. After mice were decapitated, the lower jaw, and excess tissue and bone covering the dorsal and lateral aspects of the nasal turbinates were removed. The posterior half of the brain was also removed and the remaining tissue was immersion fixed in ice-cold 4% paraformaldehyde for 2 hours at 4°C. The tissue was then decalcified for 24–48 hours in 14% ethylenediaminetetraacetic acid (EDTA) tetrasodium solution at 4°C and stored overnight in 1X phosphate-buffered saline (PBS). Wholemount X-gal staining was performed as described in Mombaerts et al. 1996 with an initial 5-hour incubation in complete β-galactosidase tissue stain solution. Tissues were then briefly rinsed in 1× PBS and fixed in 4% paraformaldehyde overnight at 4°C, before wholemounts were bisected along the medial plane following the mid-line of the brain. The staining was then performed a second time, for 4 hours, rinsed and re-fixed overnight. Wholemounts were examined using a Nikon SMZ800 dissecting microscope and images were captured using a Spot Insight IN1120 digital camera on an Olympus SZX12 stereomicroscope. The number and distribution of glomerular targeting was quantified along the medial surface prior to removal of the OB from the skull, which allowed quantification of the remaining lateral glomeruli. To quantify OSN cell bodies, multidimensional images were captured using the Instant EPI module in cellSens Standard software on a BX51 Microscope with DP70 CCD camera (Olympus). All data are presented as mean+/−S.E. Manual counts were statistically compared by Student's *t*-test, with $P<0.05$ being considered significant.

Image Analysis

Images were analyzed for area and/or fluorescence using ImageJ (Rasband,W.S., Image J, National Institutes of Health, Bethesda, Maryland, USA http://rsb.info.nih.gov/ij/, 2015). Corrected total fluorescence (CTF) was calculated using the protocol outlined by Burgess et al. 2010. Briefly, the area, integrated density, and mean gray value were measured for the glomerular layer, selected using the freeform drawing tool in ImageJ. These values were also measured for 5 background regions per image. The CTF for each image was then calculated using the following equation: CTF = Integrated Density − (Area × Mean fluorescence of

background readings). The corrected values were statistically compared to wild type by Student's *t*-test, with significance at $P<0.05$.

Results

PrP^C expression influences basal cell proliferation and survival

Transgenic mice expressing altered levels of PrP^C were used to analyze neurogenesis. Localization of PrP^C expression in the olfactory tissues of FVBCr/N mice was performed using immunohistochemistry (Fig. 1). PrP knockout (KO) mice showed no discernable PrP^C expression in any tissue (Fig. 1A and 1D), while wild type (WT) showed moderate expression in the OSE and OB, and high expression in axon bundles (Fig. 1B, E). The transgenic overexpressor (OE) mice showed increased PrP^C expression in OSE, axon bundles, and OB (Fig. 1C, F).

To analyze proliferation of newly dividing cells in the OSE, BrdU was injected intraperitoneally (i.p.) into wild type, PrP KO, and PrP OE mice and tissue was collected at 1, 7, and 14 days post-injection. After day 1 the majority of BrdU-labeled cells in the OSE were localized to the basal layer, which is consistent with BrdU incorporation into newly dividing neural progenitor cells (NPCs) (Fig. 2A and 2B). At day 7 and 14 BrdU-labeled cells were located more distal from the basal layer of the OSE and this was consistent with the migration of recently dividing NPCs towards the apical surface of the OSE and their differentiation into immature and mature neurons (Fig. 2C and 2D). BrdU-labeled cells were counted at each time point and normalized to the number of positive cells in wild type mice at day 1 post-injection. In wild type mice there was approximately a 65% reduction in BrdU-labeled cells between day 1 and day 7 ($P<0.05$), but at day 14 there was no additional reduction in cell numbers (Fig. 2E). For PrP KO mice there were a greater number of BrdU-labeled cells at day 7, but a reduced number of cells at day 14 compared to wild type mice ($P<0.05$). In contrast, in PrP OE mice there were fewer BrdU-labeled cells at day 1, but a greater number of cells at both day 7 and 14 compared to wild type mice ($P<0.05$) (Fig. 2E). These findings suggest that the absence of PrP^C does not alter basal cell proliferation, while overexpression of PrP^C can maintain mature OSN survival, which could reduce basal cell proliferation.

PrP^C maintains mature OSNs

To examine the entire neuronal population in the OSE, nasal turbinates were collected and qPCR was used to compare gene expression between wild type mice and PrP KO or PrP OE mice (Fig. 3A and 3B). The steady-state population of nascent, immature, and mature neurons in the OSE was analyzed by measuring expression of maturation stage-specific genes as well as genes that are known to regulate OSN neurogenesis (McIntyre et al. 2010, Roby et al. 2012, Shetty et al. 2005). Altering PrP levels in either PrP KO or OE mice resulted in a significant decrease in expression of two nascent OSN markers *Dbn1* (−0.092 and −0.124 log copies respectively) and *Npy* (−0.345, −0.218), but not in another, *Cxcr4* (−0.011, −0.001). A lower level of mRNA expression was also observed for the epithelium-to-mesenchyme marker *Snai2* in both PrP KO and OE (−0.141, −0.101). However, no changes in gene expression were observed in PrP KO mice for housekeeping genes (*β-actin*

[−0.029], *Eif1a* [−0.056]), markers of immature *(Gap43* [0.012] or *Dpysl3* [−0.051]) or mature OSNs *(Omp* [−0.02], *Cnga2* [0.049]), or for *Bmp4* (0.056), which inhibits the transition from immature to mature OSNs (Shou et al. 1999). Of note, one additional immature marker, axon elongation factor *IgSF8*, was downregulated (−0.138) in PrP KO animals, which may provide insight on the proposed role for PrP^C in axon outgrowth.

While PrP OE mice exhibited a significant downregulation of nascent and immature OSN markers, there was a concomitant upregulation of mature OSN gene expression compared to wild type mice (Fig. 3B). Interestingly, one immature marker, *Gap43*, was upregulated in PrP OE mice (0.129), but both markers for axonal elongation were downregulated *(IgSF8* [−0.083], *Dpysl3* [−0.226]) suggesting that maturation was incomplete. This was supported by an upregulation of *Bmp4* (0.262) whose function is to inhibit the transition of immature OSNs to the mature OSN phenotype. Despite the decrease in gene expression of early maturation markers, *Omp* and *Cnga2* are upregulated (0.151, 0.278 respectively). These findings suggest that overexpression of *Prnp* can maintain the mature OSN phenotype more effectively than wild type levels of PrP^C. This is consistent with the cell proliferation and survival data in which adult born OSNs in PrP OE mice have a longer short-term survival, which could result in a reduction of the early stages of OSN neurogenesis (Fig. 2). There was approximately a 12-fold increase in PrP OE mice as compared to wild type in the amount of mRNA for *Prnp* (1.093), the gene encoding PrP^C, and no changes in gene expression were observed for the two housekeeping genes (0.006, −0.033).

To further examine the maturation status of the OSN population within the OSE, protein analysis of GAP43 and OMP was performed in wild type mice versus PrP KO and PrP OE mice. Multiplex western blot for GAP43, OMP, and GAPDH was performed on individual nasal turbinate extracts and the signal intensity measured using LI-COR image analysis software (Fig. 4A). The GAPDH signal was used to normalize the GAP43 and OMP signal within each sample (Fig. 4B), and the ratio of immature neuron to mature OSN markers was used to calculate the relative OSN maturation status. This analysis revealed a higher amount of GAP43 in PrP OE mice with no change in OMP levels, compared to wild type mice. Examination of relative OSN maturation showed an increase of the GAP43:OMP ratio in PrP OE compared to wild type mice ($P<0.05$), but no change was found in PrP KO mice (Fig. 4C).

To determine the neuronal maturation status of only the newly divided cells in the OSE, dual immunofluorescence for BrdU and either GAP43 (i.e., immature neurons) or OMP (i.e., mature OSNs) was performed at days 7 and 14 in PrP WT, PrP KO, and PrP OE mice. Quantification of dual-labeled GAP43+BrdU cells showed PrP WT animals had 5.97 (±2.16) cells/mm at day 7, and at day 14 dual labeling decreased to 1.78 (±1.03) cells/mm (Fig. 4D, F). PrP KO animals initially had fewer dual-labeled with 4.56 cells/mm (±2.05) at day 7, but by day 14 there was no difference 1.5 (±2.16) cells/mm ($P=0.028$ and $P=0.287$, respectively). The number of dual-labeled immature cells was significantly higher in PrP OE mice as compared to PrP WT at both days 7 and 14, with 8.93 (±1.33) and 4.84 (±1.05) cells/mm, respectively ($P>0.001$). Next, quantification of dual-labeled OMP+BrdU cells showed that in PrP WT animals there was 1.05 (±0.59) mature OSNs/mm at day 7 and 1.59 (±0.68) cells/mm at day 14 (Fig. 4E, G). For mature dual-labeling there was no difference in

PrP KO as compared to wild type at either time point (P=0.31 and P=0.412). Interestingly, there were significantly fewer mature dual-labeled OSNs at both time points in PrP OE mice as compared to wild type with 0.42 (±0.24) and 0.67 (±0.31) cells/mm, at days 7 and 14 respectively, (P>0.001). This data is consistent with the whole population gene expression and protein analyses whereby, in PrP OE, newly generated OSNs are arrested in the immature neuron phenotype.

PrP^C promotes axon targeting

Immature olfactory neurons project their axons to the olfactory bulb between 4 and 8 days after division, and must make functional connections in order to be maintained and become mature OSNs (Cheetham et al. 2016). Previous *in vitro* and zebrafish studies show that PrP^C promotes cell migration, neurite formation, and axon outgrowth (Bodrikov et al. 2011, Watanabe et al. 2011, Huc-Brandt et al. 2014). We observe reduced cell survival in PrP KO animals between day 7 and 14 (Fig. 2) and altered maturation in PrP OE OSNs, in which more OSNs are arrested in the immature neuronal stage (Figs. 3, 4). Together, these data indicate that there may be changes in the ability of PrP-altered OSNs to correctly target glomeruli in the OB. To analyze whether PrP^C dose influences the final neurogenic process of axon targeting in murine OSNs, congenic P2 odorant receptor mice on a B6 background which co-express the tauLacZ reporter gene at the Olfr17 locus (P2-Olfr17$^{tm1Mom/MomJ}$) were used to measure P2 OSN axon targeting to glomeruli in the olfactory bulb. This P2 reporter line was crossed to mice with varying levels of PrP^C, quantified in both nasal turbinates and olfactory bulb by multiplex western blot (Fig. 5). For these experiments, hemizygous PrP OE animals were determined to have 4.9× the wild type level of PrP^C in the nasal turbinate, but only 2.7× in the OB. Siblings expressing only one copy of the *Prnp* gene (heterozygotes (+/−) expressed 1.2× the wild type level of PrP^C in the nasal turbinates (not statistically different), but 0.6× wild type levels of PrP^C in the OB (P<0.001). PrP WT and PrP KO animals, which have no PrP^C expression, were also used to quantify glomerular targeting of P2 OSN axons.

Prior studies have determined that P2 axons terminate on an average of 2 to 4 glomeruli per mouse olfactory bulb hemisphere (Royet et al. 1988, Mombaerts et al. 1996, Royal and Key 1999). β-galactosidase activity was used to trace P2 neurons (Fig. 6A) and their axons to both full and secondary glomeruli in the olfactory bulb. Full glomeruli were defined by a larger area with darker staining and at least 10 axon bundles coalescing to a single glomerulus, while secondary glomeruli were defined by a smaller, lighter staining area with less than 10 axons converging to a single point (Fig. 6B – 5E). In PrP WT mice, P2 axons coalesced to a mean of 2.8 full glomeruli and 2.9 secondary glomeruli for a total of 5.75 glomeruli per OB (Fig. 6D), while in PrP KO mice, these values were 4.3, 2.5, and 6.7, respectively (Fig. 6B). There was a significant increase in the number of P2 targeted full glomeruli (P<0.001) and total glomeruli (P<0.001), but not secondary glomeruli in PrP KO mice compared to PrP^C wild type mice (Fig. 6F). *Prnp* dose influences OSN axon targeting, as in PrP Het animals where there were 3.5 full, 2.3 and 5.9 total glomeruli per OB (Fig. 6C). As seen in PrP KO animals, there were significantly more full glomeruli targeted in PrP HET animals (P<0.05), but interestingly this trend was not observed in secondary or total glomerular targeting, neither of which were significantly different as compared to wild type

animals. These findings indicate that in the absence, or depletion, of *Prnp* there is a dysregulation of targeting of OSN axons to glomeruli, which could negatively affect OSN differentiation because proper integration into neural circuitry is needed for olfactory function. Finally, to examine the effect of increased PrP^C dose, quantification of glomerular targeting in PrP OE mice showed that P2 axons targeted 2.6 full glomeruli, 1.3 secondary, and 3.9 total glomeruli per OB hemisphere (Fig. 6E). This indicates a significant decrease in secondary ($P<0.001$) and total targeting ($P<0.001$) but there was no difference in full glomerular targeting as compared to wild type.

Overexpression of PrP^C refines glomerular targeting and reduces OSN axon activity

To investigate whether the observed dysregulated axon targeting in mice with altered PrP^C levels may impact the neuronal connectivity of these OSNs, we performed immunofluorescent labeling of tyrosine hydroxylase (TH) expression (Fig. 7A, B). TH labels populations of dopaminergic interneurons, whose size is correlated with OSN synaptic activity (Baker et al. 1983, Puche and Shipley 1999). In the glomerular layer of the PrP WT olfactory bulbs, there was a mean TH signal of 9.3/ mm^2. There was a trend to higher expression in the KO animals with a signal of 10.1/mm^2, but high inter-animal variation in the wild type group may have obscured significant differences. Within PrP^C overexpressing animals, TH expression was significantly reduced, to 4.05/mm^2, as compared to wild type.

Finally, to determine whether OSN number is affected by PrP^C expression, X-gal labeled P2 OSN cell bodies were quantified on a single visually accessible turbinate (turbinate IId, Liebich 1975) from the whole mounts previously used to quantify axon targeting (Fig. 7C). There were 104.2 OSNs/mm^2 in wild type animals but no significant change in P2 OSN number when PrP^C was reduced, with 95.6 cells/mm^2 in PrP KO animals and 80.6 cells/mm^2 in PrP Het animals (Fig. 7D). However, overexpression of PrP^C resulted in significant decrease in P2 cell number with 58.4 cells/mm^2 ($P<0.01$).

Discussion

PrP^C function affects rate of OSN differentiation and turnover

We have presented evidence that PrP^C is involved in the three major neurogenic processes of 1) progenitor proliferation, 2) neuronal differentiation and maturation, and 3) axon targeting, using the adult olfactory system. By examining neurogenesis across the OSN population as a whole, in a subset of OSNs (P2), and in newly-born neurons (through BrdU labeling), these studies provide a comprehensive view of the effects of PrP^C on neurogenesis and neuronal survival. The use of both PrP KO and OE transgenic mice revealed subtle trends that were essential for interpreting the roles of PrP^C in the OSE.

Previous studies on PrP KO mice confirm that these mice are viable and do have a normal lifespan while also providing examples of subtle phenotypes in neuronal function and homeostasis (Büeler et al. 1992, Manson et al. 1994, Steele et al. 2007). In fact, our data shows, not unexpectedly, that loss of PrP^C in this model has little effect on proliferation or differentiation/maturation. Loss of PrP^C initially resulted in an increased number of newborn cells surviving to 7 days, but ultimately fewer survived to 14 days post BrdU treatment. This

timing of cell loss coincides with axon targeting and integration in the OB, and therefore may be due to pruning of mistargeted axons (Kondo et al. 2010, Cheetham et al. 2016).

Previous work done either *in vitro* (Steele et al. 2006, Lee and Baskakov 2014) or in the cerebellum (Prestori et al. 2008) suggests that loss of PrP^C results in a delay of differentiation. Additionally, regeneration after mechanical injury is attenuated in PrP KO cells, and there is a delay in myogenic precursor cells exiting the cell cycle (Stella et al. 2010). Although it appears that PrP^C is important for exiting the cell cycle in muscle cells, this does not appear to translate to our *in vivo* neuronal system. Although there was decreased nascent OSN mRNA expression and fewer newborn neurons expressing the immature OSN marker GAP43, there was no difference as compared to wild type at day 14 post BrdU. Additionally, we show no difference in initial proliferation, and there was no difference in the population of immature or mature neurons as a whole by qPCR or western blot. There was also no effect of PrP KO on the ability of those newborn neurons to differentiate into OMP-expressing mature neurons at either early (7 d) or later timepoints (14 d). A more likely interpretation is that PrP^C is required to maintain the newly born cells in the OSE, and does not play a role in promoting differentiation. Therefore, this data taken together suggests compensatory mechanisms (genetic and plasticity) in proliferation and neuron maturation in a system that entirely lacks PrP^C.

Despite little effect on early neurogenesis, there is an essential role for PrP^C in appropriate target recognition within the glomerulus. The projection of axons and formation of functional synaptic connections is essential for stabilizing OSN survival (Schwob et al. 1992). Much is known about the development of a “topographical map” of glomeruli, whereby OSNs that express a single odorant receptor target a specific subset of glomeruli in the OB (reviewed in Henion and Shwarting 2007). Adult-born neurons must integrate into existing circuitry, as glomeruli are fully mature by the end of the second postnatal month (Zou et al. 2004). Although we observe mistargeting to glomeruli in PrP KO, it likely represents a stable functional circuit because it is known that PrP KO mice are capable of olfaction, despite minor behavioral deficits (Le Pichon et al. 2009). However, it remains to be seen whether this axon mistargeting is a result of an early requirement for PrP^C in development, or whether its function is needed to maintain appropriate targeting.

Many molecules and pathways, including those involving CXCR4, IGSF8, and DPYSL3 above, have been identified as being important for axon elongation, coalescence, and maintenance in the olfactory bulb (Henion and Schwarting 2007, O’Donnell et al. 2009). In fact, several known PrP-interacting proteins have been implicated to play roles these processes, including BACE1, $p75^{NTR}$, and NCAM1 (Cao et al. 2007, Cao et al. 2012, Raper and Mason 2010, Singh et al. 2008). Finding the precise molecular mechanism(s) by which PrP^C regulates OSN axon targeting will need to be carefully examined.

When attempting to ascertain the function of PrP^C, the use of PrP KO animals alone can be problematic as many previously proposed PrP KO phenotypes were later determined to arise from artifacts of the genetic background used to generate particular lines (see Wulf et al. 2017 for comprehensive review of lines and phenotypes). The “Doppel artifact,” where deletion of portions of *Prnp* exon 3 results in upregulation of the downstream prion-related

gene *Dpl* causing ataxia and Purkinje cell loss, is one such example. Although this Doppel artifact is observed in the Zurich II and Nagasaki lines, but not in the Zurich I and Edinburgh PrP KO lines used here, it is important to always control for potential artifacts. One such control, utilized in these studies, is to attempt a rescue with addition of PrP^C. The use of PrP OE mice maintained on a PrP knockout mouse background in these studies not only controls for PrP KO artifacts, but also allows us to tease apart phenotypes beyond “rescue” and reveal PrP^C dose-dependent trends.

As opposed to the dearth of knockout phenotypes, PrP^C overexpression had effects on all aspects of neurogenesis, which when viewed as a whole supports the proposed neuroprotective and pro-neuronal roles of PrP^C (reviewed in Wulf et al. 2017). Counterintuitively, proliferation in PrP OE was decreased as compared to wild type. This is as opposed to previous *in vitro* work, in which overexpression of PrP increased proliferation in multipotent neural precursors (Steele et al. 2006). However, at 14 days post-BrdU injection, when only successfully integrated, synaptically active OSNs would have survived, there were significantly more cells in the presence of excess PrP^C. Interestingly, newly-born PrP OE cells survived longer, but there were fewer total P2 OSN cell bodies, suggesting a stable mature OSN population with an increase in turnover interval. This is in contrast to another brain region that undergoes adult neurogenesis, where increased proliferation within the subventricular zone/dentate gyrus in animals overexpressing PrP^C ultimately resulted in no difference in cell number or gross morphology of these brain regions (Steele et al. 2006). The differences observed between the hippocampus and OSE may be due to different neurogenic stimulating factors within each system (such as normal OSN turnover).

Although there is less proliferation in PrP OE olfactory sensory epithelium, more of the resulting daughter cells survive seemingly arrested at the immature OSN stage. Increased GAP43 levels, by qPCR, western blot, and immunofluorescent double labeling at both 7 and 14 days post-BrdU, all show a population shift in PrP OE mice to a more immature phenotype. A decrease in expression of the axon elongation marker *Dpysl3* suggests that PrP^C regulates timing of maturation, where there are more immature OSNs but they are not projecting their axons to the OB. This inhibition of differentiation is mostly likely mediated at least partially through BMP4 (Shou et al. 1999), as we observe increased *Bmp4* expression, but whether PrP^C is directly involved in this regulation remains to be seen. Additional support for a stable mature OSN population include an increase in mature OSN mRNA levels, a concomitant decrease in nascent mRNA levels and downregulation of transition from an epithelial to mesenchymal phenotype. Together, this data supports the hypothesis that PrP^C is playing a role in maintaining individual mature OSNs, thereby inhibiting proliferation of progenitors and delaying the differentiation of immature OSNs in the olfactory sensory epithelium.

One mechanism by which PrP^C appears to be promoting OSN survival is through regulation of axon targeting. Evidence from *in vitro* and zebrafish studies demonstrates a role for PrP^C in cell migration and axon targeting (Málaga-Trillo et al. 2009, Bodrikov et al. 2011, Watanabe et al. 2011). Our data showed that increased PrP^C resulted in refined glomerular targeting by P2 OSN axons. Decreased TH expression in the glomerular layer of the OB,

along with decreased P2 OSN number, showed that overexpression of PrP^C supports proper axon targeting, thereby refining synaptic activity of OSNs, and stabilizing OSN turnover.

Conclusions

By utilizing transgenic mice with modulated PrP^C expression we further refined the role of the cellular prion protein in adult neurogenesis. This work pinpoints precise neurogenic molecular processes in which PrP^C is involved, in an *in vivo* system. Altering PrP^C level has effects on cell proliferation, neuronal differentiation and survival, as well as axon targeting. Together, they support a proneuronal role for PrP^C, whereby the presence of PrP^C promotes survival of mature neurons within the olfactory sensory epithelium.

Acknowledgments

We thank Julie Moreno for her assistance with manuscript preparation. Histological services were provided by the Experimental Pathology Facility in the College of Veterinary Medicine and Biomedical Sciences at Colorado State University. This work was supported by National Institutes of Health grant NS096662.

References

Baker H, Kawano T, Margolis FL, Joh TH. Transneuronal regulation of tyrosine hydroxylase expression in olfactory bulb of mouse and rat. J Neurosci. 1983; 3:69–78. [PubMed: 6130133]

Bessen RA, Shearin H, Martinka S, Boharski R, Lowe D, Wilham JM, Caughey B, Wiley JA. Prion shedding from olfactory neurons into nasal secretions. PLoS Pathog. 2010; 6(4):e1000837. [PubMed: 20419120]

Bessen RA, Wilham JM, Lowe D, Watschke CP, Shearin H, Martinka S, Caughey B, Wiley JA. Accelerated Shedding of Prions following Damage to the Olfactory Epithelium. J Virol. 2012; 86:1777–1788. [PubMed: 22130543]

Bodrikov V, Solis GP, Stuermer CA. Prion protein promotes growth cone development through reggie/flotillin-dependent N-cadherin trafficking. J Neurosci. 2011; 31:18013–25. [PubMed: 22159115]

Büeler H, Fischer M, Lany Y, Bleuthmann H, Lipp HP, DeArmond SJ, Prusiner SB, Aguet M, Weissmann C. Normal development and behavior of mice lacking the neuronal cell-surface PrP protein. Nature. 1992; 356:577–582. [PubMed: 1373228]

Burgess A, Vigneron S, Brioudes E, Labbé J-C, Lorca T, Castro A. Loss of human Greatwall results in G2 arrest and multiple mitotic defects due to deregulation of the cyclin B-Cdc2/PP2A balance. Proc Natl Acad Sci. 2010; 107:12564–12569. [PubMed: 20538976]

Cao L, Dhilla A, Mukai J, Blazeski R, Lodovichi C, Mason CA, Gogos JA. Genetic modulation of BDNF signaling affects the outcome of axonal competition in vivo. Curr Biol. 2007; 17:911–921. [PubMed: 17493809]

Cao L, Rickenbacher GT, Rodriguez S, Moulia TW, Albers MW. The precision of axon targeting of mouse olfactory sensory neurons requires the BACE1 protease. Sci Rep. 2012; 2:231. [PubMed: 22355745]

Cheetham CE, Park U, Belluscio L. Rapid and continuous activity-dependent plasticity of olfactory sensory input. Nat Commun. 2016; 7:10729. [PubMed: 26898529]

Dibattista M, Massimino ML, Maurya DK, Menini A, Bertoli A, Sorgato MC. The cellular prion protein is expressed in olfactory sensory neurons of adult mice but does not affect the early events of the olfactory transduction pathway. Chem Senses. 2011; 36:791–797. [PubMed: 21680753]

Farbman, AI. Cell Biology of Olfaction. Cambridge University Press; Cambridge, New York, N.Y., USA: 1992.

Gomez-Nicola D, Suzzi S, Vargas-Caballero M, Fransen NL, Al-Malki H, Cebrian-Silla A, Garcia-Verdugo JM, Riecken K, Fehse B, Perry VH. Temporal dynamics of hippocampal neurogenesis in chronic neurodegeneration. Brain. 2014; 137(Pt 8):2312–2328. [PubMed: 24941947]

Graziadei PP, Graziadei GA. Neurogenesis and neuron regeneration in the olfactory system of mammals. I. Morphological aspects of differentiation and structural organization of the olfactory sensory neurons. J Neurocytol. 1979; 8:1–18. [PubMed: 438867]

Henion TR, Schwarting GA. Patterning the developing and regenerating olfactory system. J Cell Physiol. 2007; 210:290–297. [PubMed: 17111357]

Hinds JW, Hinds PL, McNelly NA. An autoradiographic study of the mouse olfactory epithelium: evidence for long-lived receptors. Anat Rec. 1984; 210:375–383. [PubMed: 6542328]

Huc-Brandt S, Hieu N, Imberdis T, Cubedo N, Silhol M, Leighton PLA, Domaschke T, Allison WT, Perrier V, Rossel M. Zebrafish Prion Protein PrP2 Controls Collective Migration Process during Lateral Line Sensory System Development. PLoS ONE. 2014; 9(12):e113331. [PubMed: 25436888]

Kondo K, Suzukawa K, Sakamoto T, Watanabe K, Kanaya K, Ushio M, Yamaguchi T, Nibu K, Kaga K, Yamasoba T. Age-related changes in cell dynamics of the postnatal mouse olfactory neuroepithelium: cell proliferation, neuronal differentiation, and cell death. J Comp Neurol. 2010; 518:1962–1975. [PubMed: 20394053]

Lee YJ, Baskakov IV. The cellular form of the prion protein guides the differentiation of human embryonic stem cells into neuron-, oligodendrocyte-, and astrocyte-committed lineages. Prion. 2014; 8:266–275. [PubMed: 25486050]

Legname G. Elucidating the function of the prion protein. PLoS Patholog. 2017; 13(8):e1006458.

Liebich HG. Zum Bau der oberen Luftwege der weißen Ratte (Mus rattus norvegicus, var. albinos). [Structure of the upper airways of the white rat (Mus rattus norvegicus, var. albinos)]. Anat Anz. 1975; 138:170–179. [PubMed: 1217735]

Le Pichon CE, Firestein S. Expression and localization of the prion protein PrP(C) in the olfactory system of the mouse. J Comp Neurol. 2008; 508:487–499. [PubMed: 18338400]

Le Pichon CE, Valley MT, Polymenidou M, Chesler AT, Sagdullaev BT, Aguzzi A, Firestein S. Olfactory behavior and physiology are disrupted in prion protein knockout mice. Nat Neurosci. 2009; 12:60–69. [PubMed: 19098904]

Mackay-Sim A, Kittel PW. On the Life Span of Olfactory Receptor Neurons. Eur J Neurosci. 1991; 3:209–215. [PubMed: 12106197]

Málaga-Trillo E, Solis GP, Schrock Y, Geiss C, Luncz L, Thomanetz V, Stuermer CAO. Regulation of Embryonic Cell Adhesion by the Prion Protein. PLoS Biol. 2009; 7(3):e1000055.

Manson JC, Clarke AR, Hooper ML, Aitchison L, McConnell I, Hope J. 129/Ola mice carrying a null mutation in PrP that abolishes mRNA production are developmentally normal. Mol Neurobiol. 1994; 8:121–127. [PubMed: 7999308]

McIntyre JC, Titlow WB, McClintock TS. Axon Growth and Guidance Genes Identify Nascent, Immature, and Mature Olfactory Sensory Neurons. J Neurosci Res. 2010; 88:3243–3256. [PubMed: 20882566]

McLean IW, Nakane PK. Periodate-lysine-paraformaldehyde fixative. A new fixation for immunoelectron microscopy. J Histochem Cytochem. 1974; 22:1077–1083. [PubMed: 4374474]

Mehrabian M, Brethour D, Wang H, Xi Z, Rogaeva E, Schmitt-Ulms G. The Prion Protein Controls Polysialylation of Neural Cell Adhesion Molecule 1 during Cellular Morphogenesis. PLoS ONE. 2015; 10(8):e0133741. [PubMed: 26288071]

Mombaerts P, Wang F, Dulac C, Chao SK, Nemes A, Mendelsohn M, Edmondson J, Axel R. Visualizing an olfactory sensory map. Cell. 1996; 87:675–686. [PubMed: 8929536]

Murray RC, Calof AL. Neuronal regeneration: lessons from the olfactory system. Semin Cell Dev Biol. 1999; 10:421–431. [PubMed: 10497099]

O'Donnell M, Chance RK, Bashaw GJ. Axon growth and guidance: receptor regulation and signal transduction. Annu Rev Neurosci. 2009; 32:383–412. [PubMed: 19400716]

Parrie LE, Renfrew EM, Vander Wal A, Mueller RL, Garrity DM. Zebrafish tbx5 paralogs demonstrate independent essential requirements in cardiac and pectoral fin development. Dev Dyn. 2013; 242:485–502. [PubMed: 23441045]

Prestori F, Rossi P, Bearzatto B, Lainé J, Necchi D, Diwakar S, Schiffmann SN, Axelrad H, D'Angelo E. Altered neuron excitability and synaptic plasticity in the cerebellar granular layer of juvenile

prion protein knock-out mice with impaired motor control. J Neurosci. 2008; 28:7091–7103. [PubMed: 18614678]

Puche AC, Shipley MT. Odor-induced, activity-dependent transneuronal gene induction *in vitro*: mediation by NMDA receptors. J Neuro. 1999; 19:1359–1370.

Raper J, Mason C. Cellular Strategies of Axonal Pathfinding. Cold Spring Harb Perspect Biol. 2010; 2(9):a001933. [PubMed: 20591992]

Roby YA, Bushey MA, Cheng LE, Kulaga HM, Lee SJ, Reed RR. Zfp423/OAZ mutation reveals the importance of Olf/EBF transcription activity in olfactory neuronal maturation. J Neurosci. 2012; 32(40):13679–88a. [PubMed: 23035080]

Royal SJ, Key B. Development of P2 olfactory glomeruli in P2- internal ribosome entry site-tau-LacZ transgenic mice. J Neurosci. 1999; 19:9856–9864. [PubMed: 10559395]

Royet JP, Souchier C, Jourdan F, Ploye H. Morphometric study of the glomerular population in the mouse olfactory bulb: numerical density and size distribution along the rostrocaudal axis. J Comp Neurol. 1988; 270:559–568. [PubMed: 3372747]

Schaefer ML, Finger TE, Restrepo D. Variability of position of the P2 glomerulus within a map of the mouse olfactory bulb. J Comp Neurol. 2001; 436:351–362. [PubMed: 11438935]

Schwob JE, Szumowski KE, Stasky AA. Olfactory sensory neurons are trophically dependent on the olfactory bulb for their prolonged survival. J Neurosci. 1992; 12:3896–3919. [PubMed: 1403089]

Shetty RS, Bose SC, Nickell MD, McIntyre JC, Hardin DH, Harris AM, McClintock TS. Transcriptional changes during neuronal death and replacement in the olfactory epithelium. Mol Cell Neurosci. 2005; 30:90–107. [PubMed: 16027002]

Shou J, Rim PC, Calof AL. BMPs inhibit neurogenesis by a mechanism involving degradation of a transcription factor. Nat Neurosci. 1999; 2:339–345. [PubMed: 10204540]

Singh KK, Park KJ, Hong EJ, Kramer BM, Greenberg ME, Kaplan DR, Miller FD. Developmental axon pruning mediated by BDNF-p75NTR-dependent axon degeneration. Nat Neurosci. 2008; 11:649–658. [PubMed: 18382462]

Steele AD, Emsley JG, Ozdinler PH, Lindquist S, Macklis JD. Prion protein (PrP^C) positively regulates neural precursor proliferation during developmental and adult mammalian neurogenesis. Proc Natl Acad Sci U S A. 2006; 103:3416–3421. [PubMed: 16492732]

Steele AD, Lindquist S, Aguzzi A. The prion protein knockout mouse: a phenotype under challenge. Prion. 2007; 1:83–93. [PubMed: 19164918]

Stella R, Massimino ML, Sandri M, Sorgato MC, Bertoli A. Cellular prion protein promotes regeneration of adult muscle tissue. Mol Cell Biol. 2010; 30:4864–4876. [PubMed: 20679477]

Watanabe T, Yasutaka Y, Nishioku T, Kusakabe S, Futagami K, Yamauchi A, Kataoka Y. Involvement of the cellular prion protein in the migration of brain microvascular endothelial cells. Neurosci Lett. 2011; 496:121–124. [PubMed: 21511010]

Wulf MA, Senatore A, Aguzzi A. The biological function of the cellular prion protein: an update. BMC Biol. 2017; 15:34. [PubMed: 28464931]

Zanusso G, Ferrari S, Cardone F, Zampieri P, Gelati M, Fiorini M, Farinazzo A, Gardiman M, Cavallaro T, Bentivoglio M, Righetti PG, Pocchiari M, Rizzuto N, Monaco S. Detection of pathologic prion protein in the olfactory epithelium in sporadic Creutzfeldt-Jakob disease. N Engl J Med. 2003; 348:711–9. [PubMed: 12594315]

Zou DJ, Feinstein P, Rivers AL, Mathews GA, Kim A, Greer CA, Mombaerts P, Firestein S. Postnatal refinement of peripheral olfactory projections. Science. 2004; 304:1976–1979. [PubMed: 15178749]

Highlights

1. The cellular prion protein is neuroprotective in olfactory neurogenesis.
2. Prion knockout impacts axon targeting but not neuronal composition.
3. Prion overexpression maintains mature neurons thereby reducing adult neurogenesis.
4. Prion overexpression refines olfactory neuron axon targeting.

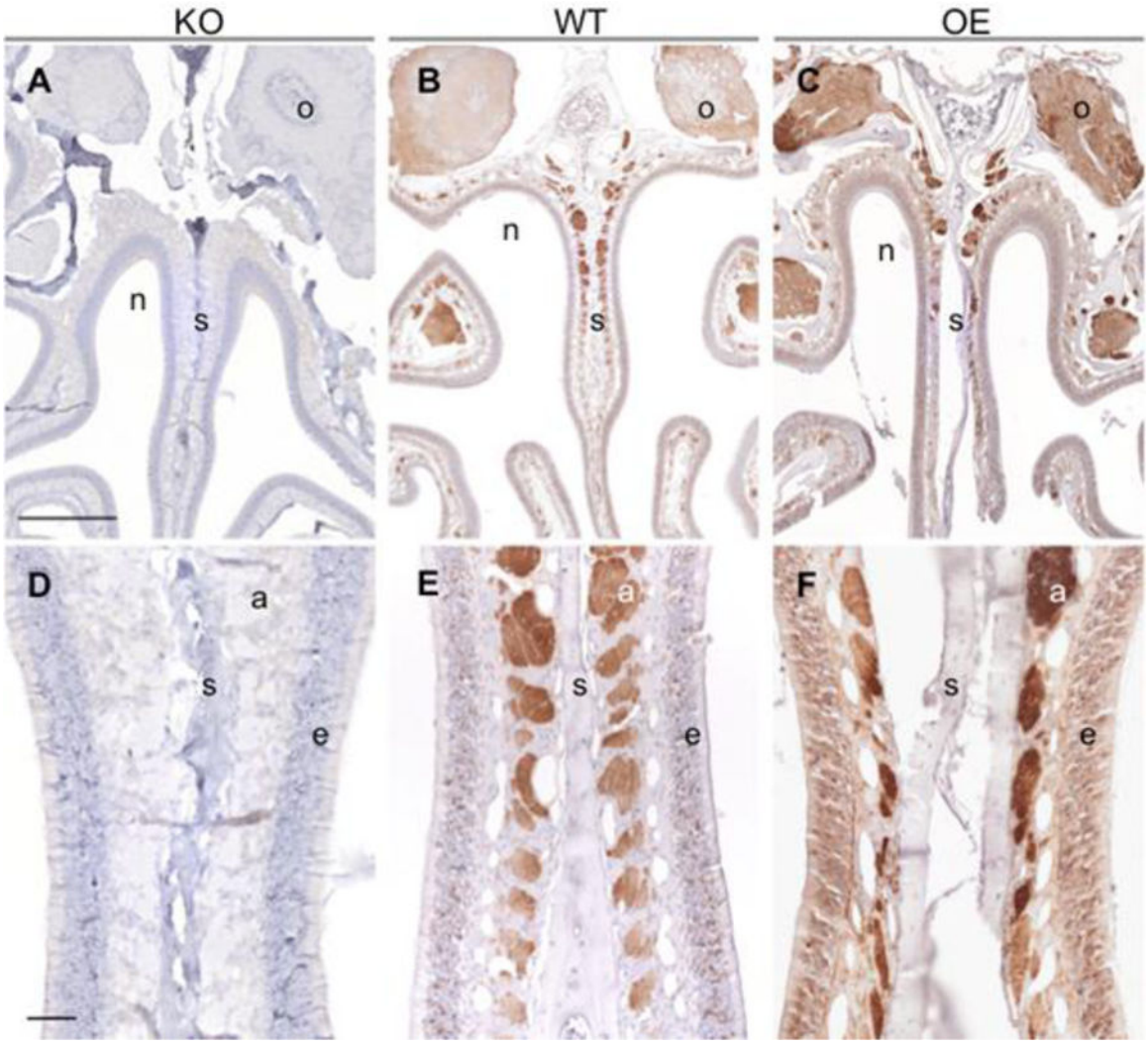

Figure 1.

PrP^C expression in murine olfactory tissues. Representative micrographs of immunohistochemical staining for PrP^C in coronal sections from PrP knockout (KO; *A, D*), wild type (WT; *B, E*), and overexpressor (OE; *C,F)* FVB/N mice. (*D-F*) higher magnification images of the septum (s) area from each genotype. a: axon bundles; e: olfactory sensory epithelium; n: nasal cavity; o: olfactory bulb; s: septum. Scale bars: (A)=500μm, (D)=50μm.

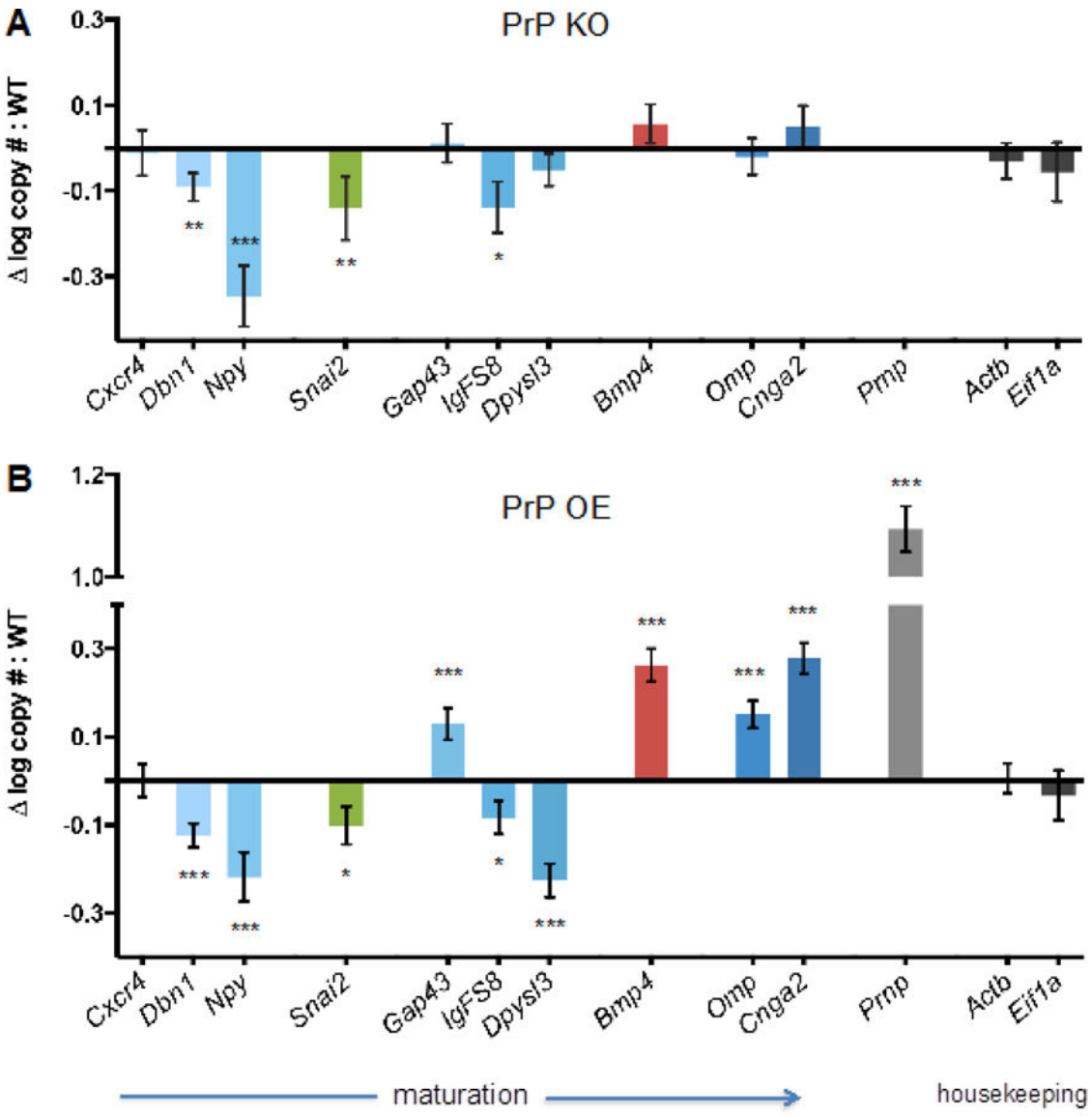

Figure 2.

Proliferation and survival of BrdU-labeled cells within the OSE is PrP^C dependent. OSE demonstrating cellular proliferation at 1 day post BrdU injection (*A*). Mitotically active cells are labeled with BrdU (brown) and the tissue is counterstained with hemotoxylin (blue). (*B*) BrdU incorporation at day 1 with no counterstain. BrdU-labeling also shows migration of newly divided cells within the epithelium as well as cell survival to 7 (*C*) and 14 (*D*) days post BrdU injection. Scale bar: 25 μm. (*E*) Quantification of BrdU labeled cells in the OSE (mean ±S.E.M., with statistical significance at $*P<0.05$ by two-way ANOVA (n=3)).

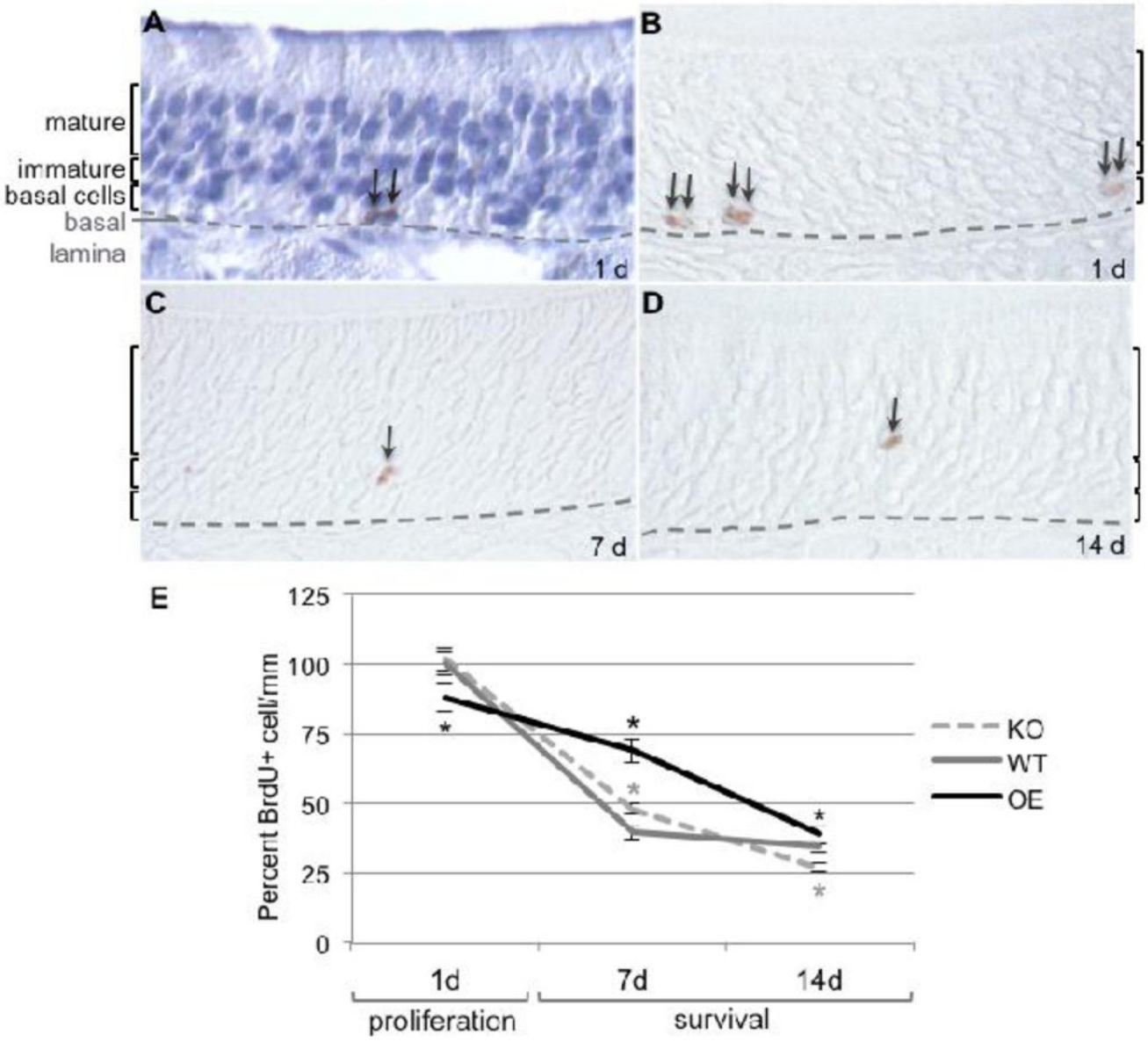

Figure 3.

Effect of PrP^C on OSN differentiation and maturation marker gene expression. Quantitative PCR analysis of gene expression of developmental stage-specific markers (blue bars) and signaling molecules that promote (*Snai2*, green) or inhibit (*Bmp4*, red) neuronal maturation under normal conditions. Housekeeping genes *Actb* and *Eif1a* were also analyzed to determine if gene expression was equivalent between genotypes. Data is represented as change in total log copy number as compared to wild type and analyzed by Student's *t*-test, where * $P<0.05$, ** $P<0.01$, *** $P<0.001$ (mean ± standard error of the difference between means, n=8).

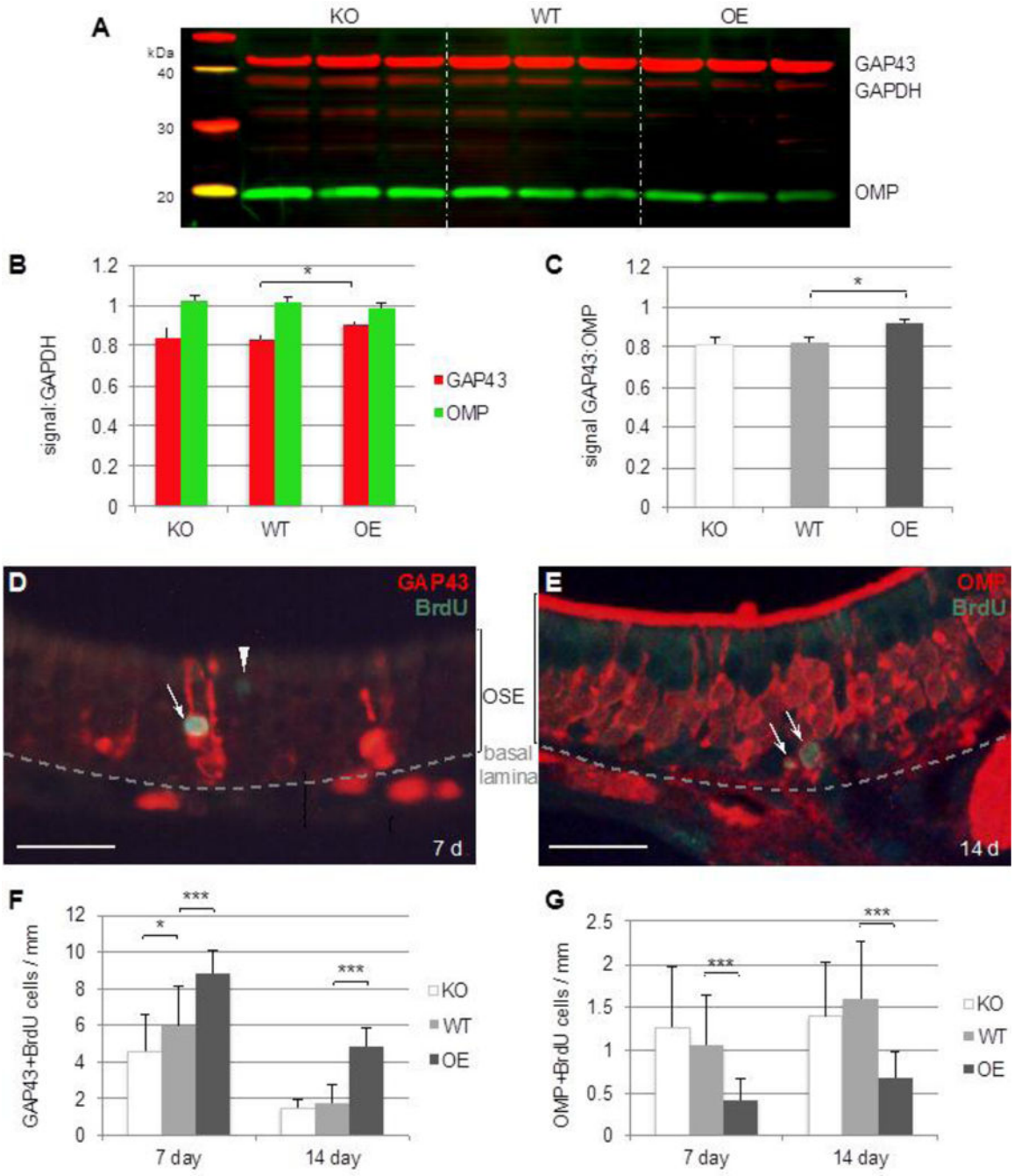

Figure 4.

PrP^{C} expression level alters timing of olfactory sensory neuron differentiation. Representative image of multiplexed western blot of maturation markers (GAP43 in red at 43 kDa and OMP in green at 19 kDa) and GAPDH (red bands at 38 kDa, to establish protein amounts loaded) in whole nasal turbinate homogenates (*A*). (*B*) Quantification of maturation marker protein signals normalized to GAPDH. (*C*) Determination of the relative OSN maturation state for each PrP^{C} genotype in which the ratio of the log-transformed immature marker signal was divided by that of the mature signal, (n=6). *(D, E)* Representative overlay

micrographs of OSE demonstrating dual-labeling of BrdU+ nuclei (green) and maturation markers (red) for immature neurons (GAP43, *D*) and mature neurons (OMP, *E*). Arrows: location of dual-labeled cells. Arrowhead: BrdU-lableled nucleus which does not co-localize with the maturation marker. Scale bars: 25 μm. Quantification of cells dual-labeled with BrdU and GAP43 (*F*) or OMP (*G*) in the OSE, (n=3). All quantification shown as mean ± S.E.M, and was analyzed by Student's *t*-test, statistical significance at $*P<0.05$, $***P<0.001$.

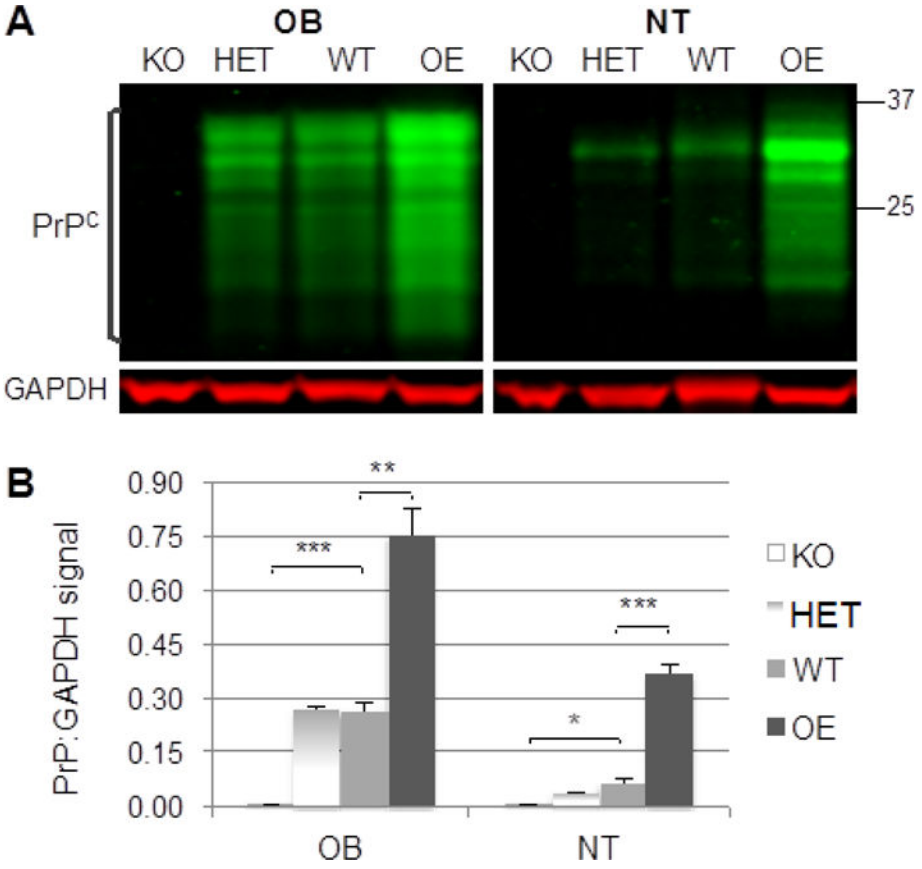

Figure 5.

PrP^C expression levels in P2 transgenic murine olfactory tissues. Representative multiplex western blots (*A*) for protein expression in the nasal turbinate (NT) or olfactory bulb (OB) homogenates to confirm PrP^C expression in peripheral tissues of P2 transgenic mice using D18 anti-PrP and GAPDH antibodies. (*B*) Quantification of total PrP^C signal from 18 to 37 kDA was normalized to GAPDH for each animal (n=3, HET, OE), compared to WT (n=5) shown as mean ± S.E.M. and analyzed by Student's *t*-test with significance at $*P<0.05$, $**P<0.01$, $***P<0.001$.

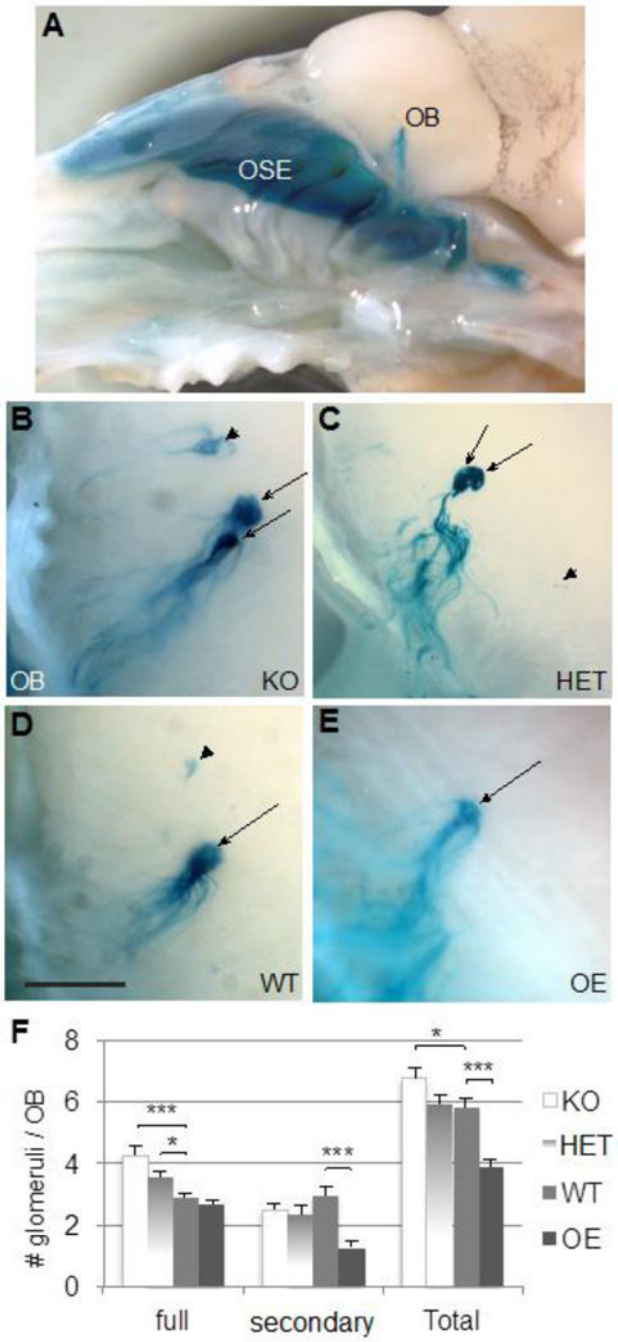

Figure 6.

Axon targeting to P2 glomeruli in the olfactory bulb (OB) is PrP^C dose-dependent. (*A*) Low magnification view of X-gal staining of P2 neurons in the OSE and OB. (*B-E*) X-gal staining of axons converging onto glomeruli with the OB of mice with increasing amounts of PrP^C expression. Scale bar: 500μm. (*F*) Quantification of glomeruli staining (mean ± S.E.M., KO n=14, HET n=8, WT n=13, OE n=12). Arrows: full glomeruli; arrowhead: secondary glomeruli. Significance at * $P<0.05$, *** $P<0.001$ when compared to wild type by Student's *t*-test.

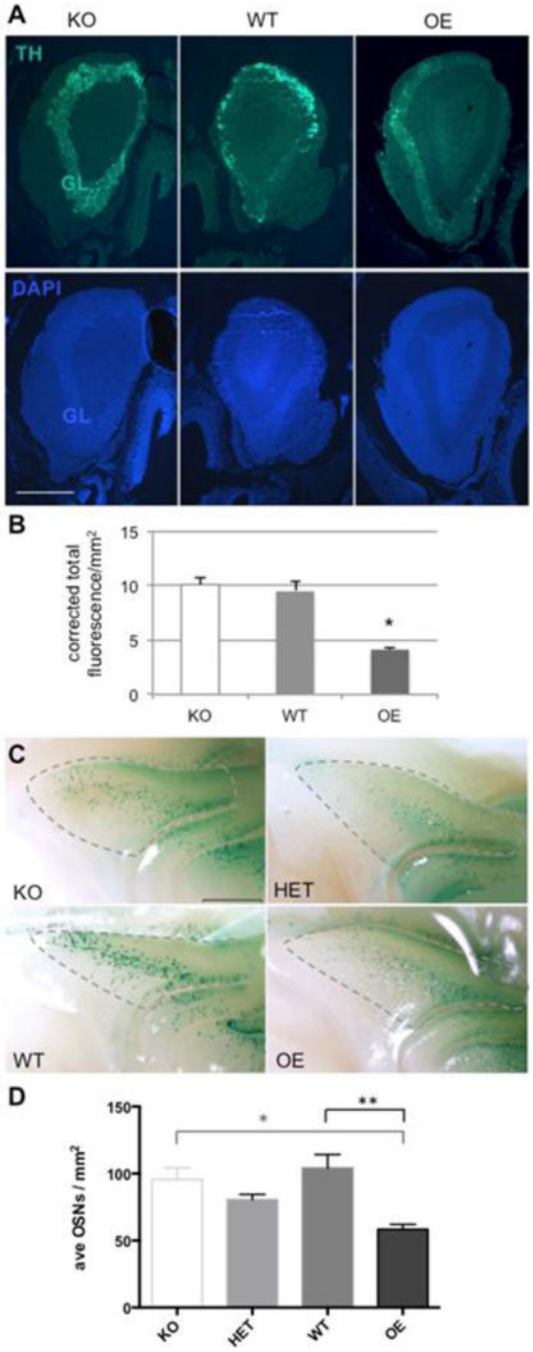

Figure 7.

Overexpression of PrP^C results in decreased OSN synaptic activity and reduced OSN number. (*A*) Representative images of coronal OB sections with immunofluorescence staining for tyrosine hydroxylase (TH, green) in the glomerular layer for each *Prnp* genotype. TH activity in dopaminergic interneurons increases in an OSN-activity dependent manner. Lower panels show the nuclear stain (dapi, blue) for each OB in corresponding panel above. Scale bar: 500 μm. (*B*) Quantification of mean TH immunofluorescent labeling (±S.E.M.), with statistical significance by Student's *t*-test:WT at **P*<0.05 (n=4 KO, WT;

n=5 OE). (*C*) X-gal stained P2 neurons in the OSE from transgenic animals with increasing levels of PrP^{C}. Only the labeled OSNs in the upper medial nasal turbinate were visualized for quantification (area outlined in gray). Scale bar: 500 μm. (*D*) Quantification of P2 OSN cell bodies, analyzed by ANOVA with significance at $*P<0.05$, $**P<0.01$ (KO n=21, HET n=9, WT n=20, OE n=11).